SLAC-PUB-13583
April 2009

A Ball Lightning Model as a Possible Explanation of Recently Reported Cavity Lights*

David Fryberger**
SLAC National Accelerator Laboratory
2575 Sand Hill Road, MS 20
Stanford University
Menlo Park, California 94025 USA

Abstract

The salient features of cavity lights, in particular, mobile luminous objects (MLO's), as have been experimentally observed in superconducting accelerator cavities, are summarized. A model based upon standard electromagnetic interactions between a small particle and the 1.5 GHz cavity excitation field is described. This model can explain some features of these data, in particular, the existence of particle orbits without wall contact. While this result is an important success for the model, it is detailed why the model as it stands is incomplete. It is argued that no avenues for a suitable extension of the model through established physics appear evident, which motivates an investigation of a model based upon a more exotic object, ball lightning. As discussed, further motivation derives from the fact that there are significant similarities in many of the qualitative features of ball lightning and MLO's, even though they appear in quite different circumstances and differ in scale by orders of magnitude.

The ball lightning model, which incorporates electromagnetic charges and currents, is based on a symmetrized set of Maxwell's equations in which the electromagnetic sources and fields are characterized by a process called dyality rotation. It is shown that a consistent mathematical description of dyality rotation as a physical process can be achieved by adding suitable (phenomenological) current terms to supplement the usual current terms in the symmetrized Maxwell's equations. These currents, which enable the conservation of electric and magnetic charge, are called vacuum currents.

It is shown that the proposed ball lightning model offers a good qualitative explanation of the perplexing aspects of the MLO data. Avenues for further study are indicated.

PACS: 46.90 + s; 52.80 Mg
Keywords: Field emission; cavity lights, ball lightning

*Work Supported by Department of Energy Contract DE-AC02-76SF-00515
**Tel. +1-650-926-2768, e-mail: *fryberger@slac.stanford.edu*

Submitted to Nuclear Instrumentation and Methods (NIM)

I. INTRODUCTION

The observation of very unusual luminous phenomena taking place inside of electrically energized superconducting niobium rf cavities has been reported [1]. This observation was accomplished using a small video camera looking through a standard vacuum viewport along the axis of the cavity mounted in a 2K liquid helium bath inside of a test facility dewar. (Hence, there is no electron beam in the experimental set up, and the vacuum inside the cavity is very good.) There is no evidence to support the notion that the lights are some artifact of optics or the camera. In fact, upon examination of the totality of the data, one is forced to conclude that the luminosity emanates from small objects, generally ≤ 1.5 mm in size, that are not attached to the cavity walls but rather are freely moving about in the vacuum inside of the cavity. In this regard, perhaps the most persuasive aspect of the data is the fact that in many sequences consistent frame-by-frame reflections of the tracks of the objects can be seen in the walls of the cavity, affording a quasi-stereo view of the objects, and clearly indicating that the moving objects are, in general, not in contact with the cavity wall. Hence, these objects have been called Mobile Luminous Objects or MLO's.

One of the most interesting aspects of the observations is the existence of long-lived closed orbits, which implies that the MLO's carry a certain mass and that they are subject to a centrifugal force. It follows that this centrifugal force must be matched by some (inward) radial force. Further analysis of the data reveals that there are also clear multiframe sequences of tracks, complete with confirming reflections, in which the objects are actually seen to bounce off of the cavity wall, indicating that they have a certain integrity and self-coherence. This motion (i.e., the orbits and wall bounces) can be characterized as ballistic, in which single MLO's move about in the vacuum space of the cavity obeying, to first order, Newton's equations of motion. In Ref [2] this was called Mode I behavior.

Subsequent experimental results, discussed in some detail in Ref. [2], have made even more difficult a proper physical explanation of the phenomena. In this data set, the MLO's are seen to remain at rest (or in slow motion) for more than a minute inside the cavity (presumably) in or near the equatorial plane. Furthermore, in some segments of this data there are multiple MLO's (as many as seven), visible simultaneously, occupying the vertices of a (quasi-stationary) polygonal pattern, which pattern was likened to a macromolecule. The objects and this pattern are sometimes observed to move in a slow and coherent circular rotation about the cavity axis, all rotating together maintaining to first order the polygonal pattern as an invariant. As a second order modification to this behavior, the MLO's have relative motions within the pattern, and in one instance two objects appear to exchange places (but without actual contact) on adjacent vertices of the polygonal pattern. Thus, the data of Ref. [2] show that not only do the MLO's interact with the walls, they can settle into a stable equilibrium formation away from the walls. Furthermore, the MLO's can also interact with

each other, and at a distance that considerably exceeds their apparent size, as already suggested by the data of Ref. [1]. In Ref. [2] these qualitatively different, non-ballistic aspects were categorized as Mode II behavior.

In the sections that follow, we summarize some salient characteristics of MLO's; explore a Small Particle Model (SPM) [3], which can explain some aspects of observed MLO behavior; invite a comparison of MLO's to some salient characteristics of ball lightning (BL); and formulate a BL model based upon a symmetrized set of Maxwell's equations. In this formulation, which explicitly includes magnetic charge and current, the symmetry between electricity and magnetism is called dyality symmetry [4], and the model exploits dyality symmetry in a fundamental way. Finally, it is shown that this model can explain some of the more perplexing aspects of MLO's (and BL), as observed, and some predictions are made.

II. SALIENT CHARACTERISTICS OF MLO's

1) Luminosity is observed, evidently from a small object, which we shall denote by MLO.

2) MLO's can move about inside the cavity for extended periods of time (many seconds) without any wall contact.

3) This motion exhibits stability in an empty volume of three dimensional space, which calls for some unknown long range force.

4) Multiple MLO's can interact with each other at long range. And this interaction must be able to develop a potential well for particle pairs that exhibits a minimum at a distance considerably exceeding the apparent size of the MLO's.

5) The MLO's can have a lifetime of a minute or more, far too long for conventional plasma in a vacuum without wall contact.

6) The long lifetime implies that if the objects are some new kind of plasma then a self-coherence force is required to hold the MLO together.[1] (Calculations based upon the SPM, discussed below, indicate that MLO's are of too low a density to be a normal solid or liquid.)

7) The MLO's have been observed to bounce off of the cavity walls, further demonstrating their self-coherence.

One must keep in mind that these aspects of the MLO data have been observed on several occasions and are in need of a proper physical explanation.

[1]The mathematics of this assertion is contained in the virial theorem [5, 6].

III. SMALL PARTICLE MODEL

The SPM was developed in an effort to try to understand the MLO phenomenon. This model uses standard electromagnetic theory (*e.g.*, Jackson [7]) to calculate the Lorentz $\boldsymbol{v}\times\boldsymbol{B}$ force that derives from the electromagnetic (accelerating) fields (of frequency f_a = 1.5 GHz) in the cavity. (Boldface type denotes three-vectors.) This force results from the fact that the rf $\boldsymbol{E}$ field in the cavity induces in a small particle a 1.5 GHz oscillating electric dipole moment $\boldsymbol{\mu}$, which in turn interacts with the rf $\boldsymbol{B}$ field. Hence, the $\boldsymbol{v}$ is not the particle velocity, but rather the internal electric charge velocity associated with the oscillating dipole moment. Assuming that an MLO could be modeled by a conducting sphere of radius a, it was shown that this force $\boldsymbol{F}$ is proportional to the radial distance ρ of the particle from the cavity axis and is directed inward along that radius. That is [3, Eq. (7)],

$$\boldsymbol{F} = -\frac{E_0^2\omega_a^2\rho a^3\mathbf{1}_\rho}{4c^2}, \tag{1}$$

where E_0 is the peak electric field in the center of the cavity, $\omega_a = 2\pi f_a$, and c is the velocity of light. Note that Eq. (1) is in Gaussian units, which will be used throughout this paper.

The force given by Eq. (1) is that of a cylindrical harmonic potential well, which has as general solutions elliptical orbits about the cavity axis. Since (quasi) elliptical orbits were observed, this result is an important success of the model. However, if one accepts that the $\boldsymbol{v}\times\boldsymbol{B}$ force is dictating the particle orbits, it is still clear from the data that the model is incomplete; the observed orbits wobble, rock, deform, and in general assume a large variety of shapes, showing that there must be additional forces at play.

Another major deficiency of the model was also pointed out: due to the inherent curvature of the off-axis $\boldsymbol{E}$ field, the cylindrical trapping force leads at the same time to a force promoting an axial instability with a time constant τ_{ai} scaled by the inverse of the orbital frequency f_o, which for the data of Ref. [1] fell in the range of $5 \le f_o \le 80$ Hz. The fact that in four instances observed orbits lasted longer than 10 s (estimated to be 125 τ_{ai} in one instance [3][2]) indicates that a more complete model will require some force to overcome this instability. But an examination of other possibilities in established physics, which included image forces, the pondermotive force, and gravitation, revealed no viable candidates for such a force [3].

The axial stability question is made even more perplexing by the data reported in Ref. [2], in which the objects remained for many minutes in the cavity volume away from the cavity walls. For this data, it would appear that the force leading

[2] The longevity of these orbits found in the initial data was noted but not emphasized in Ref. [1], which was a fairly brief report.

to axial stability is also dominating the putative $\boldsymbol{v}\times\boldsymbol{B}$ force: the macromolecules are neither in contact with the cavity walls (where image forces could be relevant), nor on axis, which is the location of the potential minimum defined by Eq. (1).

The SPM has another interesting result. For closed orbits of a conducting[3] sphere, it yields for the orbital frequency f_o the formula [3, Eq. (9)]

$$f_o = \frac{\omega_o}{2\pi} = \frac{E_0 f_a}{4c}\sqrt{\frac{3}{\pi\rho_M}}, \tag{2}$$

where ρ_M is the mass density of the sphere. Thus, if the SPM assumptions are satisfied, a measurement of the orbital frequency in the data of Ref. [1] yields a measurement of the density of an orbiting sphere. (It is argued below that a sphere is an appropriate shape with which to model MLO.) That is,

$$\rho_M = \frac{3E_0^2 f_a^2}{16\pi f_o^2 c^2}. \tag{3}$$

A sample calculation was made for an observed 80 Hz orbit yielding ρ_M~1.7 mg/cm^3, roughly that of air, which at STP is ~1.2 mg/cm^3. Even allowing for the uncertainty (of perhaps a factor of two) in the value of E_0, one concludes that known solid (or liquid) materials are too heavy[4] to be trapped by the Lorentz force into an 80 Hz orbit. At the same time this calculation shows that any conventional plasma (which might somehow exist in the cavity vacuum) would be too light to be consistent with the SPM as formulated in Ref. [3].

It should be mentioned here that special geometries, i. e., a very thin spherical shell or a long needle (aspect ratio of 300), were shown to be able to circumvent the density criterion posed above for solids; these geometries offer a much larger induced electric moment per unit mass. (A liquid, of course, could not stably maintain itself as a hollow sphere or a long needle.) Although it is unlikely that such objects would be found in the clean, high-vacuum environment of the superconducting niobium cavities, the crucial objection is that they offer no plausible basis on which to overcome the axial instability problem and hence cannot offer a real solution to the question of the nature of the observed MLO's. This latter problem, then, is the main reason for not looking to special geometries or structures[5] as viable objects with which to model MLO's.

---

[3] In the SPM, the particle can be either a conductor or a dielectric, but for dielectrics having reasonable dielectric constants possible agreement with the data is untenable.

[4] This result also eliminates the very low density “solids," such as styrofoam or aerogel, even if they would be good conductors; they are also too heavy.

[5] This line of reasoning also argues that novel proposed ball lightning structures such as a tangle of fractal fibres [8], nano-particle networks [9], or a tangle of polymer threads [10] are not viable as models for MLO's.

In summary, the SPM offers important, yet limited insights. The assumption that the $\boldsymbol{v} \times \boldsymbol{B}$ force explains (to lowest order) the orbital forces on an MLO rules out the known states of matter: solid, liquid, gas, or plasma. (A Bose-Einstein condensate is too fragile and too light to be viable.) And an additional problem applies to the gas or plasma concept. Even if a plasma (or gas) cloud could somehow satisfy the density requirement, one is required to find a force that could hold such a cloud together for the extended observation times of ≥ 10 s, or, more stringently, as in the case of the data of Ref. [2], for coherence times of a minute or more. In addition, there is no evident extension of the SPM that might explain the large variety of observed MLO motion.

We are thus presented with a dilemma. If we accept the SPM as valid, we are confronted with questions that do not appear to have answers within the realm of established physics. What is the nature of these objects? What are the forces acting on them? On the other hand, if we reject the SPM as not relevant, we are left with even more questions as to the nature of MLO's and even less, *i.e.*, essentially nothing, to go on. As a path out of this dilemma, our view is to accept the approach taken in the SPM as a suitable first step. That is, look to electromagnetism, the only available long range force, for an understanding of the MLO phenomena. After all, electromagnetism and the electromagnetic properties of matter have universal applicability. (Gravitation, though universal, is much too weak to be considered relevant here.)

As the next step, building upon the ideas in the SPM, we consider another phenomenon that has also defied explanation by established physics: ball lightning, or BL. A significant motivation for this step comes from the striking similarities between MLO and BL characteristics, as indicated in the next section. A second motivation is that the particular BL model we have in mind [11] incorporates magnetic charge as an intrinsic feature. It is argued below that magnetic charge, as incorporated into the above-sited BL model, can explain the observed axial stability of the MLO orbits. This step, of course, is speculative, but it would appear that the nature of the data in hand calls for an exploration outside the realm of established physics.

IV. SALIENT ASPECTS OF BALL LIGHTNING

BL is a phenomenon that is generally associated with thunderstorms [12-15]. Some salient aspects that are particularly relevant to this study are listed below.

1) BL exhibits significant luminosity with no evident source of energy. (Actually, the energy supply for the MLO luminosity probably derives from the cavity rf field.)

2) It floats in the air, free of any connection to material objects, obviously too light to be a conventional solid or liquid.

3) It is subject to long range forces, as it tends to avoid walls or other objects and to pass through openings, such open windows or doors.

4) It is sometimes observed in multiples, mutually orbiting each other [12, 16].

5) It is long-lived, with reliable observations of up to 1 min or more, too long to be a conventional hot gas or plasma.

6) The coherence of BL as a well-defined energetic luminous object for such extended periods is an apparent violation of the virial theorem.[6]

7) It has been observed to roll or bounce along the ground, furnishing further evidence of self-coherence.

8) It is seen in a variety of colors: red, orange, yellow, and white being the most common.[7]

At the present time, there are many proposed explanations for BL, but it is fair to say that as of yet none has gained general acceptance. One of the major difficulties to achieving an understanding of BL is that there is very little proper technical data available; it is a rather rare natural phenomenon, and so far no one has been able to convincingly produce it in the laboratory.

It is also worth mentioning here that another (rare) phenomenon known as earth lights, or EL [18, 19], has also been observed to exhibit many of the same features (with the exception of the third and seventh for which there are insufficient data). EL are large luminous objects, a meter or (possibly much) more in size, that are observed moving about the sky. Sometimes they are very long-lived, with durations of one or more hours [18]. We wish to emphasize here that we view EL as a natural (luminous) physical phenomenon that, while (unfortunately) included in the UFO category, has nothing to do with alien spacecraft and the like.

It is indeed intriguing, then, that we are presented with three distinct yet similar phenomena on widely differing scales: MLO's on a scale of 1 mm or less, BL on the cm to meter scale [20], and EL on a scale of a meter to many meters. In view of their similarities in behavior and general characteristics (except for scale), we adopt the working hypothesis that these phenomena are manifestations of essentially the same physics, and that the explanation for one can furnish a path to an explanation for the other two. Consequently, we now look at the cavity lights phenomenon in the framework of a specific BL model [11].

---

[6] Endean [17] has emphasized this point to the ball lightning community.

[7] The apparent colors of MLO's are not yet known as all optical data to date have been obtained using a monochrome video camera.

V. BALL LIGHTNING MODEL

A. Generalities

The fundamental equations of our BL model are Maxwell's equations [21] using a two-potential approach [22] generalized to manifest full symmetry between electricity and magnetism. This symmetry, which has been known for over a century [23], is sometimes called duality symmetry. However, we follow Han and Biedenharn [4] who use the term "dyality" to avoid any confusion associated with other uses of the term "duality." As pointed out by Rainich [24], the dyality symmetry of Maxwell's equations is a continuous symmetry which may be parameterized by an angle Θ, which we call the dyality angle. Using a form of Hamilton's principle, a Lagrangian formulation has been derived [25] that simultaneously yields the dyality symmetric set of Maxwell's equations and the dyality symmetric Lorentz force equation, affording this theoretical framework a more secure footing. This BL model, which exploits dyality symmetry in an essential way, is based on an object called the vorton [26]. And the BL itself is in essence a collection of a large number of vortons in a state of coherent dyality rotation.[8]

B. The Vorton

The vorton is a (static) semiclassical monopole configuration of electromagnetic charge and its associated electromagnetic fields that satisfy the dyality symmetric set of Maxwell's equations. In qualitative terms, the vorton is a quantized vortex and as such is viewed as a fundamental electromagnetic object. For the convenience of the reader, the attributes and a brief description of the vorton are given below.

The vorton sustains two quantized internal circulations,[9] one about the z-axis carrying an angular momentum associated with the operator L_ϕ, and one of a toroidal nature (motion like a smoke ring) associated with L_ψ, a toroidal angular momentum operator. The z components of L_ϕ and L_ψ can be simultaneously diagonalized. The (rotational) symmetries implied by these angular momenta devolve from the conformal invariance of Maxwell's equations [29, 30]. The structure and geometry of the vorton are best described using a (right-handed) toroidal coordinate system (σ, ψ, ϕ) [31]. A schematic depiction of the vorton

[8] It is relevant to point out that the vorton of this model, as described in Ref. [26] is a fundamental electromagnetic object; it is not the same as the cosmic vorton [27], which evolved out of studies of cosmic strings. A fairly comprehensive discussion of cosmic vortons, which are closed cosmic strings or loops, can be found in Ref. [28].

[9] We use the term "circulation" here to indicate a sense of flow or current flux lines, but without actual motion; the electromagnetic charge distribution is smooth and continuous, and the vorton solution is a static or dc configuration of this charge in which no intrinsic feature varies with time. Viewing the vorton solution as a static configuration obviates the need for any consideration of internal superluminal motion. And one can still use the (static) electromagnetic equations.

structure is given in Fig. 1. This figure, which is adapted from Penrose and Rindler [32], demonstrates that vorton structure bears a close relationship to (a projection of) the twistor. (Both are based upon conformal invariance.)

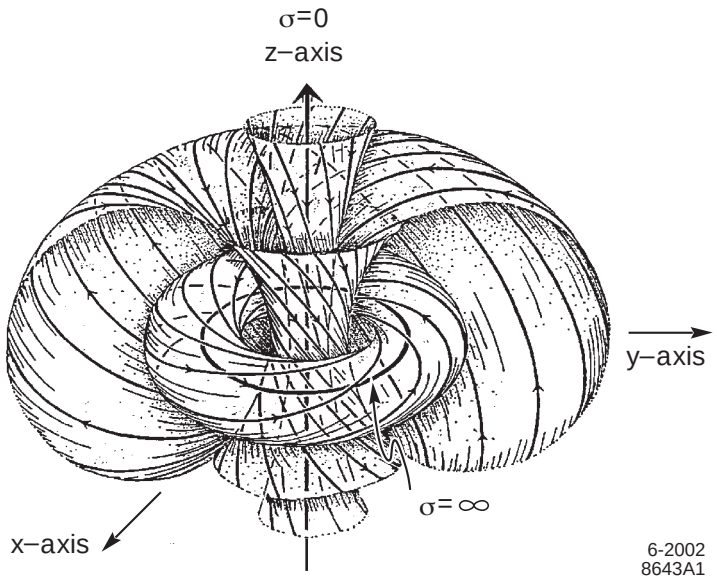

Figure 1: Schematic depiction of the structure of the vorton. The basic underlying toroidal coordinate system is evident. The arrows denote the simultaneous "rotations" or charge flux lines in ϕ and ψ, which are associated with L_ϕ (around the *z*-axis or $\sigma = 0$) and L_ψ (around the ring of radius *a*, *i.e.*, $\sigma = \infty$, which sets the scale of the toroidal system). One can see that the charge flux lines, as indicated by the arrows, all lie in the surface of one of the (nested) tori and are in the sense of increasing ϕ and ψ. By definition, this configuration carries positive topological charge.

The vorton ground state carries an electromagnetic charge of magnitude Q_0 and one unit each of L_ϕ and L_ψ; *i.e.*, L_ϕ and L_ψ have eigenvalues $\pm\hbar$, where $\hbar$ is the (reduced) Planck constant. Since L_ϕ and L_ψ are nonzero, the vorton also carries a unit of topological or Hopf charge, which renders the vorton absolutely stable, although pair production and annihilation are possible. Q_0 is set by a (semi-classical) quantum condition on L_ϕ and L_ψ, and satisfies the equation

$$\frac{Q_0^2}{\hbar c} = 2\pi\sqrt{\frac{3}{5}} \cong 4.867. \tag{4}$$

Using the phenomenological relationship

$$\frac{e^2}{\hbar c} \cong \frac{1}{137}, \tag{5}$$

where *e* is the positron charge, yields

$$Q_0 \cong 25.83e. \tag{6}$$

It is acknowledged that this is not the well-known value of the Dirac monopole charge [33] ~ 68.5*e*.[10] In general, then, the electric and magnetic charges on a vorton are given by $Q_0\cos\Theta$ and $Q_0\sin\Theta$, respectively, where each vorton can carry its own Θ with reference to a fixed set of electromagnetic axes.[11] Gaussian units enable the direct display of the dyality symmetry between electricity and magnetism; in Gaussian units the vacuum constitutive parameters are $\mu_0 = \epsilon_0 = 1$. Fig. 2 depicts a general vorton charge in the electromagnetic plane.

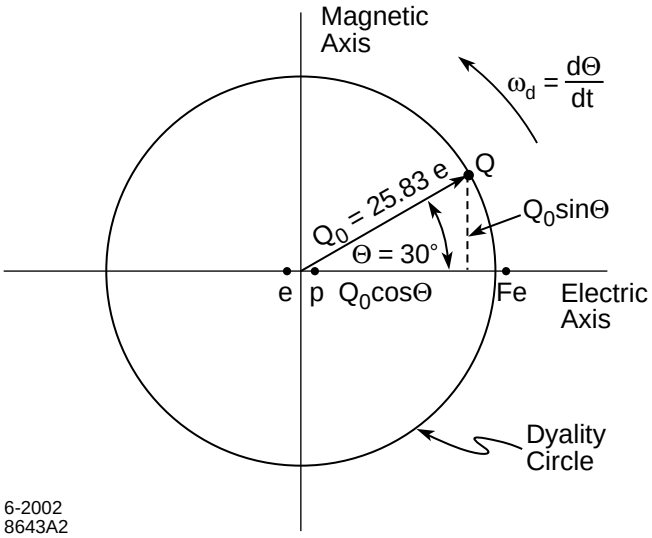

Figure 2: The electromagnetic or dyality plane with electric and magnetic axes is shown. The circle of radius Q_0 (equivalent to 25.83 *e*), the magnitude of the (ground state) vorton's generalized electromagnetic charge, is also shown. This circle is called the dyality circle, and any point on this circle, designated by its dyality angle Θ, is a possible value for the vorton charge. A $Q = Q_0$ at $\Theta = 30°$ is indicated. For orientation, the electron *e*, the proton *p*, and the iron nucleus Fe ($Z = 26$) are plotted. If the vorton charge is in a state of dyality rotation of angular velocity ω_d, then $\omega_d = d\Theta/dt$, as depicted in the figure.

The mass of the vorton is entirely electromagnetic and has been shown [26] to be

$$m_v = \frac{5Q_0^2}{2\pi a_v c^2}, \tag{7}$$

where a_v is the scale of the vorton's toroidal coordinate system. Since there is no intrinsic scale associated with classical electromagnetism, the vorton, as a purely

[10] It is argued in Ref. [25] that in the case of the two-potential approach and for unbound particles the Dirac quantum condition between electric and magnetic charge does not obtain. It is also shown in the approach taken in Ref. [25] that there are no Dirac strings attached to magnetic monopoles.

[11] This fixed reference set of electromagnetic axes could be furnished by the quantum vacuum, or Dirac sea; it would be defined throughout spacetime by a pair of scalar functions $\Theta_{0_e}(x^\mu)$ and $\Theta_{0_m}(x^\mu)$.

electromagnetic object, has no intrinsic scale. Rather, the scale (and hence the mass) of any given vorton would be determined by the details of its production process. Half of m_v is associated with the monopole charge Q_0, and half with the circulation of charge, *i.e.*, with L_ϕ and L_ψ. In turn, the half due to circulation is equally divided between the circulations associated with L_ϕ and L_ψ. By dyality symmetry, m_v is invariant with respect to Θ.

C. Vorton Production

In the case of BL, it is postulated that the constituent vortons are pair produced by the lightning stroke itself. Since the diameter of the current path is on the order of a centimeter, the characteristic scale of these vortons would be on the order of a centimeter. In the case of MLO's, it is assumed that the vorton production process involves field emission.[12] Two field emission processes may contribute: 1) there appear to be sites of steady field emission, which are assumed to be associated with the observed stationary points of light on the cavity iris, and 2) there are also observed to be bright flashes of duration ~ 1 ms, often preceding the appearance of cavity lights. This second category appears to be associated with the explosive destruction of field emission sites [35]. (One is tempted to draw an analogy between these bright flashes and the lightning stroke.) Based upon studies of the effective area of field emission sites [34], the field emission assumption would imply that the constituent vortons of MLO's would be of a scale ranging from 3×10^{-3} down to 10^{-7} cm.

The produced vortons in both of these processes would carry electric charge but no magnetic charge. That is, they would be characterized by $\Theta = 0$ or π. The passage from a large collection of electric vorton pairs produced by a stroke of lightning (or by field emission) to a stable BL (or MLO) involves a dyality spinup process.[13] After spinup, MLO's, BL, and EL would be characterized by a physical process that we call dyality rotation. While the essential physics of the fully formed MLO's, BL, or EL after dyality spinup would be the same,[14] due to different environments and scales, one expects there to be differences in some physics details.

---

[12] Like lightning, field emission is transient in the sense that its electron flow is abruptly interrupted (with a frequency of f_a). Also the activity of the MLO phenomenon subsides in roughly an hour and does not return, consistent with what is known about the "processing" of field emission sites [34, 35].

[13] It is assumed that every lightning stroke produces a large quantity of vorton pairs, but the reason that BL is so rare in nature is that the dyality spinup process depends upon a number of variables each of which needs to be in the right range and with the right timing for the process to reach fruition.

[14] On the other hand, the physics details of the dyality spinup processes for BL, MLO's, and EL will differ and will be covered elsewhere.

D. Dyality Rotation by a Fixed Angle

Dyality rotation needs dyality symmetric Maxwell's equations for a proper description. The development of the dyality symmetric Maxwell's equations is well known. However, for the convenience of the reader we sketch it here to furnish a basis for a better understanding of the physical dyality rotation of electromagnetic charges and currents, which calls for a nontrivial extension of the physics of these equations. The first step is to write the standard set of Maxwell's equations for (the macroscopic fields of) electromagnetism [7, p. 178]:

$$\nabla \cdot \boldsymbol{D} = 4\pi\rho_e, \qquad \nabla \times \boldsymbol{H} = \frac{4\pi}{c}\boldsymbol{j} + \frac{1}{c}\frac{\partial \boldsymbol{D}}{\partial t}, \tag{8}$$

and

$$\nabla \cdot \boldsymbol{B} = 0, \qquad -\nabla \times \boldsymbol{E} = \frac{1}{c}\frac{\partial \boldsymbol{B}}{\partial t}. \tag{9}$$

The $\partial \boldsymbol{D}/\partial t$ term in Eq. (8) is the famous displacement current added by Maxwell [21]. One obtains the analogous Maxwell's equations for magneto-electricity by using the dyality symmetry exchange substitutions [4, 36]:

$$(\rho_e, \boldsymbol{j}, \boldsymbol{E}, \boldsymbol{D}) \Rightarrow \pm(\rho_m, \boldsymbol{g}, \boldsymbol{H}', \boldsymbol{B}'), \tag{10}$$

and

$$(\boldsymbol{H}, \boldsymbol{B}) \Rightarrow \mp(\boldsymbol{E}', \boldsymbol{D}'), \tag{11}$$

where the primes are used to denote the magneto-electric field quantities, and ρ_m and $\boldsymbol{g}$ are magnetic charge and vector current densities, respectively. Eqs. (10 and 11) are accompanied by the "inverse" substitutions

$$(\rho_m, \boldsymbol{g}, \boldsymbol{H}', \boldsymbol{B}') \Rightarrow \mp(\rho_e, \boldsymbol{j}, \boldsymbol{E}, \boldsymbol{D}), \tag{12}$$

and

$$(\boldsymbol{E}', \boldsymbol{D}') \Rightarrow \pm(\boldsymbol{H}, \boldsymbol{B}). \tag{13}$$

Applying Eqs. (10 and 11), with the upper sign on the right hand side, to Eqs. (8 and 9) yields

$$\nabla \cdot \boldsymbol{B}' = 4\pi\rho_m, \qquad -\nabla \times \boldsymbol{E}' = \frac{4\pi}{c}\boldsymbol{g} + \frac{1}{c}\frac{\partial \boldsymbol{B}'}{\partial t}, \tag{14}$$

and

$$-\nabla \cdot \boldsymbol{D}' = 0, \qquad -\nabla \times \boldsymbol{H}' = -\frac{1}{c}\frac{\partial \boldsymbol{D}'}{\partial t}, \tag{15}$$

the appropriate magneto-electric equations. (The minus sign in Eq. (14) indicates that the $\boldsymbol{E}'$ field generated by $\boldsymbol{g}$ obeys a left hand rule.) One can now combine Eqs. (14 and 15) with Eqs. (8 and 9) to obtain a dyality symmetric set of Maxwell's equations:

$$\nabla\bullet(\boldsymbol{D}+\boldsymbol{D}')=4\pi\rho_e,\qquad \nabla\times(\boldsymbol{H}+\boldsymbol{H}')=\frac{4\pi}{c}\boldsymbol{j}+\frac{1}{c}\frac{\partial(\boldsymbol{D}+\boldsymbol{D}')}{\partial t},\qquad (16)$$

and

$$\nabla\bullet(\boldsymbol{B}'+\boldsymbol{B})=4\pi\rho_m,\qquad -\nabla\times(\boldsymbol{E}'+\boldsymbol{E})=\frac{4\pi}{c}\boldsymbol{g}+\frac{1}{c}\frac{\partial(\boldsymbol{B}'+\boldsymbol{B})}{\partial t},\qquad (17)$$

where we have separately included the symbols for both the electromagnetic and magneto-electric quantities. (In this picture, magneto-electric fields are physically distinguishable from electromagnetic fields; they differ in parity; *cf.* Ref. [25].)

Conservation of charge is easy to demonstrate. First take the divergence of the second equation of Eqs. (16 and 17) to obtain

$$0=\frac{4\pi}{c}\nabla\bullet\boldsymbol{j}+\frac{1}{c}\nabla\bullet\frac{\partial}{\partial t}(\boldsymbol{D}+\boldsymbol{D}'),\qquad (18)$$

and

$$0=\frac{4\pi}{c}\nabla\bullet\boldsymbol{g}+\frac{1}{c}\nabla\bullet\frac{\partial}{\partial t}(\boldsymbol{B}'+\boldsymbol{B}),\qquad (19)$$

where we have used, *e.g.*, $\nabla\bullet\nabla\times\boldsymbol{H}=0$. Interchanging the order of ∇ and $\partial/\partial t$ in Eqs. (18 and 19) and then using the first equation of Eqs. (16 and 17) yields

$$0=\nabla\bullet\boldsymbol{j}+\frac{\partial\rho_e}{\partial t},\qquad (20)$$

and

$$0=\nabla\bullet\boldsymbol{g}+\frac{\partial\rho_m}{\partial t}.\qquad (21)$$

That is, electric and magnetic charge are conserved separately.

We now introduce the fact that dyality symmetry (or invariance) of the set of generalized Maxwell's equations is a continuous symmetry parameterized by Θ, which specifies a rotation of the electromagnetic plane. This rotation, illustrated in Fig. 3a, leads to a new decomposition of the charges, currents, and fields:

$$\begin{aligned}\rho_e^R&=\rho_e\cos\Theta-\rho_m\sin\Theta,\\ \rho_m^R&=\rho_e\sin\Theta+\rho_m\cos\Theta,\\ \boldsymbol{j}^R&=\boldsymbol{j}\cos\Theta-\boldsymbol{g}\sin\Theta,\end{aligned}\qquad (22)$$

and

$$\boldsymbol{g}^R=\boldsymbol{j}\sin\Theta+\boldsymbol{g}\cos\Theta$$

for the charges and currents, and

$$\begin{aligned} \mathcal{D}^R &= \mathcal{D}\cos\Theta - \mathcal{B}\sin\Theta, \\ \mathcal{B}^R &= \mathcal{D}\sin\Theta + \mathcal{B}\cos\Theta, \\ \mathcal{E}^R &= \mathcal{E}\cos\Theta - \mathcal{H}\sin\Theta, \end{aligned} \tag{23}$$

and

$$\mathcal{H}^R = \mathcal{E}\sin\Theta + \mathcal{H}\cos\Theta$$

for the field quantities, where for notational convenience the definitions

$$\mathcal{D} \equiv \boldsymbol{D} + \boldsymbol{D}', \ \mathcal{B} \equiv \boldsymbol{B} + \boldsymbol{B}', \ \textit{etc.} \tag{24}$$

have been used. One sees that the dyality exchange substitutions of Eqs. (10 - 13) are special cases of dyality rotation specified by $\Theta = \pm\pi/2$.

Applying Eqs. (22-24) to Eqs. (16 and 17) and collecting the terms in the rotated electromagnetic coordinate system again yields a dyality symmetric set of Maxwell's equations, *i.e.*, Eqs. (16 and 17), but, of course, after the dyality rotation. Hence, a discrete dyality rotation by Θ will change the terms to describe the physical processes, but does not change the physical processes themselves.[15] Equivalently, one can rotate (in the opposite direction) the physical electromagnetic quantities by an angle Θ, leaving the electromagnetic plane fixed, as illustrated in Fig. 3b.

To proceed, let us consider the initial condition for the simplest physical situation that would be relevant to a MLO'S, BL, or EL, namely a localized electric charge density distribution ρ_{0_e} at the origin with no magnetic charge and no currents. We label with the subscript 0 these initial quantities. This system will satisfy the dyality invariant set of Maxwell's equations:

$$\nabla\cdot\mathcal{D}_0 = \nabla\cdot(\boldsymbol{D}_0 + \boldsymbol{D}_0') = 4\pi\rho_{0_e}, \qquad \nabla\times\mathcal{H}_0 = \frac{1}{c}\frac{\partial\mathcal{D}_0}{\partial t}, \tag{25}$$

$$\nabla\cdot\mathcal{B}_0 = \nabla\cdot(\boldsymbol{B}_0' + \boldsymbol{B}_0) = 0, \qquad -\nabla\times\mathcal{E}_0 = \frac{1}{c}\frac{\partial\mathcal{B}_0}{\partial t}, \tag{26}$$

where, anticipating the dyality rotation, we have explicitly decomposed $\mathcal{D}_0$ and $\mathcal{B}_0$ in the left hand equations. In these equations, only the field quantity $\boldsymbol{D}_0$ and the electron charge density ρ_{0_e} are nonzero. For this static configuration, the right hand equations are null. ($\boldsymbol{E}_0$ is nonzero, but $\nabla\times\boldsymbol{E}_0 = 0$ for the static Coulomb field.) Using Eqs. (22 and 23) to rotate the source and fields in Eqs. (25 and 26) by the (fixed) dyality angle Θ yields:

[15] For example, it can be said that we might just as well have taken the electron (and proton, etc.) to be magnetically charged, or even some mixture of electric and magnetic charge, *e.g., cf.* Ref. [37] or [38].

$$\nabla \cdot \mathcal{D}_0^R = \nabla \cdot \boldsymbol{D}_0 \cos\Theta = 4\pi\rho_{0_e}^R = 4\pi\rho_{0_e} \cos\Theta, \tag{27}$$

$$\nabla \cdot \mathcal{B}_0^R = \nabla \cdot \boldsymbol{D}_0 \sin\Theta = 4\pi\rho_{0_m}^R = 4\pi\rho_{0_e} \sin\Theta, \tag{28}$$

$$\nabla \times \mathcal{H}_0^R = \nabla \times \boldsymbol{E}_0 \sin\Theta = \frac{1}{c}\frac{\partial \mathcal{D}_0^R}{\partial t} = \frac{1}{c}\frac{\partial}{\partial t}(\boldsymbol{D}_0 \cos\Theta), \tag{29}$$

and

$$-\nabla \times \mathcal{E}_0^R = -\nabla \times \boldsymbol{E}_0 \cos\Theta = \frac{1}{c}\frac{\partial \mathcal{B}_0^R}{\partial t} = \frac{1}{c}\frac{\partial}{\partial t}(\boldsymbol{D}_0 \sin\Theta), \tag{30}$$

where we have used the fact that $\mathcal{B}_0 = \mathcal{H}_0 = 0$. Having rotated the charge and fields, the original electric charge is now comprised of electric and magnetic components specified by ρ_{0_e} and Θ. The magnetic components of charge are, of course, associated with the appropriate (Coulomb) magnetic fields, although designated here in terms of the initial electric fields (before rotation). With a fixed Θ, Eqs. (27-30) represent from a physical point of view the same initial conditions as do Eqs. (25 and 26). As before, Eqs. (29 and 30) are null.

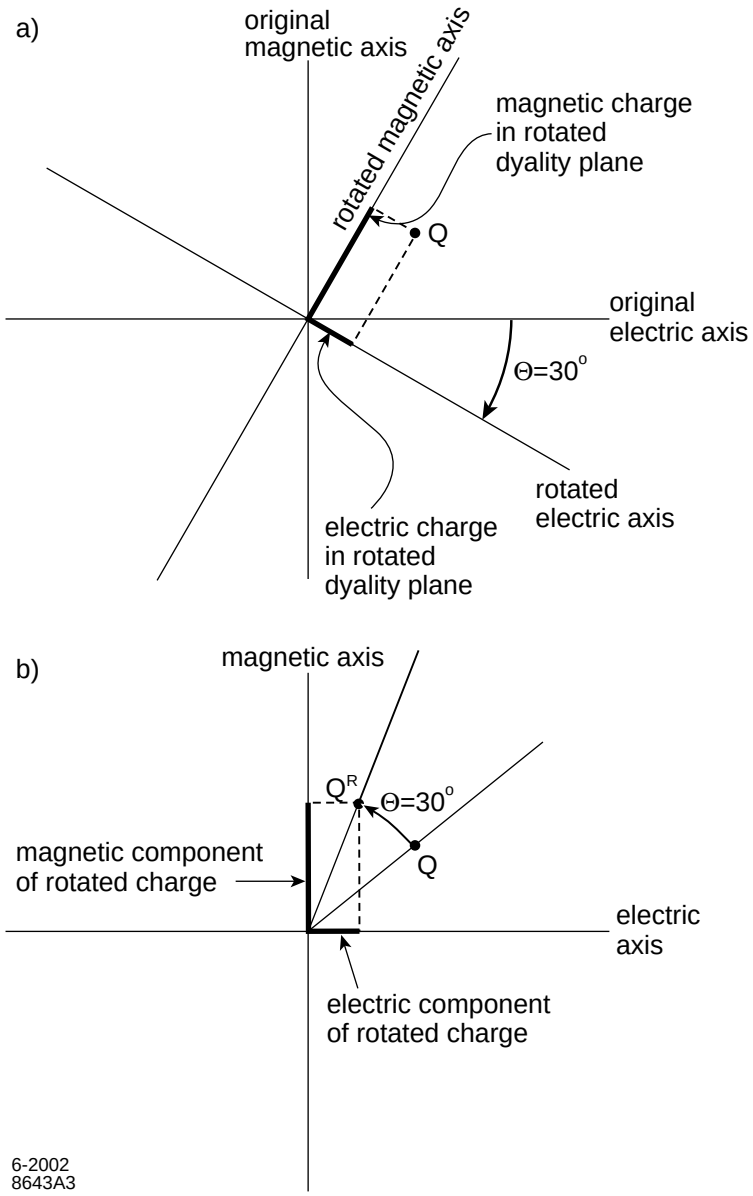

Figure 3: a.) Illustration of the rotation of the electromagnetic plane by the angle Θ = 30°. The same charge Q has new electromagnetic components in the rotated plane. b.) Rotation of electromagnetic charge by the same angle Θ = 30°. The rotated charge Q^R has new electromagnetic components in the (same) dyality plane.

E. Dyality Rotation as a Dynamical Process

In order to consider dyality rotation as a dynamical physical process, we set

$$\Theta = \omega_d t \tag{31}$$

where ω_d is the (angular) frequency of dyality rotation. Eqs. (27-30) then become

$$\nabla \cdot \mathcal{D}_0 \cos\omega_d t = 4\pi\rho_{0_e} \cos\omega_d t \equiv 4\rho_e(t) \tag{32}$$

$$\nabla \cdot \mathcal{D}_0 \sin\omega_d t = 4\pi\rho_{0_e} \sin\omega_d t \equiv 4\rho_m(t) \tag{33}$$

$$\nabla \times \mathcal{E}_0 \sin\omega_d t = \frac{1}{c}\frac{\partial}{\partial t}(\mathcal{D}_0 \cos\omega_d t), \tag{34}$$

and

$$-\nabla \times \mathcal{E}_0 \cos\omega_d t = \frac{1}{c}\frac{\partial}{\partial t}(\mathcal{D}_0 \sin\omega_d t), \tag{35}$$

all of which are explicitly time dependent.

At once we see that there are problems. Not only is charge not conserved in Eqs. (32 and 33), but both Eq. (34) and Eq. (35) cannot be satisfied because $\nabla \times \mathcal{E}_0 = 0$ on the left hand side and the time derivative on the right hand side is now nonzero. To address these problems and obtain a consistent mathematical description of the dyality rotation process, there are (at least) two possible approaches: 1) assume, as Maxwell did, that there is some term missing from the symmetrized Maxwell's equations, or 2) assume that there is some new and unrecognized physical process, as was done, for example, to explain the missing energy in beta decay. Following the latter approach, we postulate that there are new kinds of electromagnetic currents present, which we shall call vacuum currents $\boldsymbol{j}_v$ and $\boldsymbol{g}_v$.

Assuming that the process of dyality rotation generates (these new phenomenological) vacuum currents, then Eqs. (34 and 35) are rewritten as

$$\nabla \times \mathcal{E}_0 \sin\omega_d t = \frac{4\pi}{c}\boldsymbol{j}_v + \frac{1}{c}\frac{\partial}{\partial t}(\mathcal{D}_0 \cos\omega_d t), \tag{34′}$$

and

$$-\nabla \times \mathcal{E}_0 \cos\omega_d t = \frac{4\pi}{c}\boldsymbol{g}_v + \frac{1}{c}\frac{\partial}{\partial t}(\mathcal{D}_0 \sin\omega_d t). \tag{35′}$$

Eqs. (34′ and 35′) may be solved to give

$$\boldsymbol{j}_v(t) = \frac{\omega_d}{4\pi}\mathcal{D}_0 \sin\omega_d t \tag{36}$$

and

$$\boldsymbol{g}_v(t) = \frac{\omega_d}{4\pi}\boldsymbol{\mathcal{D}}_0 \cos\omega_d t, \tag{37}$$

resolving the problem introduced by the time dependent dyality angle in Eqs. (34 and 35). Proceeding as above in the derivation of Eqs. (19 and 20), taking the divergence of Eqs. (34′ and 35′), yields

$$0 = \nabla\cdot\boldsymbol{j}_v + \frac{\partial\rho_e}{\partial t} \tag{38}$$

and

$$0 = \nabla\cdot\boldsymbol{g}_v + \frac{\partial\rho_m}{\partial t}, \tag{39}$$

which shows that the postulation that there are vacuum currents also leads to the conservation of electric and magnetic charge separately, as before. Taking the divergence of Eqs. (36 and 37), we deduce that

$$\frac{\partial\rho_e(t)}{\partial t} = -\omega_d\rho_m(t) \tag{40}$$

and

$$\frac{\partial\rho_m(t)}{\partial t} = \omega_d\rho_e(t), \tag{41}$$

which is consistent with the condition of dyality rotation as depicted in Fig. 2.

Note that the vacuum currents flow radially into and out of the charge distribution undergoing dyality rotation. In this picture, if one assumes that the vacuum currents implied by dyality rotation are flowing and are subsumed in the usual electric and magnetic current terms, then the symmetric set of Maxwell's equations, *i.e*., Eqs. (16 and 17), gives a complete description of electromagnetic phenomena including dyality rotation. Thus, the mathematics is the same, but the scope of the physics is augmented. (The introduction of vacuum currents constitutes an update to the original BL discussion given in Ref [11]).

It should be mentioned that ascribing these currents to a vacuum process implies that they do not depend upon ordinary matter to flow.[16] That is, since the quantum vacuum or Dirac sea is populated at the maximum density allowed by the Pauli exclusion principle, the presence or nonpresence of matter is essentially irrelevant; the particle density in the Dirac sea exceeds that of ordinary matter by many orders of magnitude. In looking for a physical basis for these vacuum currents, one can imagine that the quantum vacuum could carry perturbations in the dyality reference angles, mentioned above, as waves in spacetime. Since the $\Theta_{0_e}(x^\mu)$ and $\Theta_{0_m}(x^\mu)$ are scalar functions, these spacetime waves would be

[16] With regard to the vacuum currents proposed here, it is of interest to review Maxwell's thinking about displacement currents. For example, *cf.* Ref. [39].

governed by the Klein-Gordon equation; this picture suggests that the mass term in that equation would be $m_{0_d} = \hbar / (\lambda\!\!\!^{-}_{0_d} c)$, where $\lambda\!\!\!^{-}_{0_d}$ is discussed below.

One expects these proposed vacuum currents to have physical effects, generating $\boldsymbol{H}$ or $\boldsymbol{E}'$ fields, respectively, as dictated by the generalized (and extended) Maxwell's equations. As described below, detection of these effects should be experimentally accessible.

F. Qualitative Description of the MLO/BL/EL Configuration

At this point, it is useful to give a qualitative description of the fully formed MLO/BL/EL configuration after dyality spinup, which by observation is a relatively long-lived stable equilibrium configuration localized in space. The central feature of such configurations is, in this model, a large number of vortons characterized by coherent dyality rotation. We shall call this the vorton core, and assume it contains N_v vortons. In addition to N_v, other features characterizing the vorton core are its size, its dyangular momentum (described below), the mean size (or more generally the size distribution function) of its constituent vortons, and the kinetic temperature (see below) of its vortons. The kinetic temperature will depend upon the heating mechanism for the MLO/BL/EL, and can be viewed as a phenomenological parameter.

The oscillating electric charge of the vorton core will attract or repel electrons and ions according to the (common) value of Θ. In addition, ionization of the neutral atoms entrained in the vorton core will also be a source of electrons and ions in the core. Thus, in general, MLO'S, BL, and EL consist of a plasma of vortons, electrons, and ions as well as entrained neutral atoms. Among these several features, there are two parameters that are independent and (essentially) constant: N_v and dyangular momentum. These two primary parameters are fundamental in the description of MLO/BL/EL. For the complete characterization of MLO/BL/EL these are supplemented by the size of the core,[17] the kinetic temperature, the vorton size distribution, and a description of the local environment. Thus, one sees that the vorton model entails a two (plus) dimensional parameter space in which to contain the phenomena of MLO, BL, and EL. We now turn to the physics of the vorton core, which is the driving engine of the MLO/BL/EL configuration(s).

[17] As indicated by Eq. (51) below, if the kinetic temperature is negligible, the size of the vorton core is, in principle, derivable from N_v and the dyangular momentum.

G. The Vorton Core

1. Electromagnetic Energy

It was stated above that the electromagnetic energy of an individual vorton is proportional to Q_0^2 and is equally divided between that due to the monopole of charge and that due to circulation. To evaluate the electromagnetic energy of the vorton core, we observe that the N_v vortons of the core are in a state of coherent dyality rotation. That is, they are localized in space (at the origin, say) and occupy the same (rather small) region of the (Θ, ω_d) phase space.[18] (That an equilibrium configuration will manifest these features will be justified below.) Thus, each of these N_v vortons will have (essentially) the same electric and magnetic charge components, and the vorton core will be characterized by a monopole of electromagnetic charge of magnitude N_vQ_0 undergoing coherent dyality rotation at the frequency ω_d. The Coulomb energy E_c of this (macroscopic) monopole configuration is independent of Θ and is given by

$$E_c = \frac{(N_v Q_0)^2}{R_c}, \tag{42}$$

where R_c is the (effective) radius of the core. We make the assumption that the (L_ϕ and L_ψ) circulation axes of the N_v vortons in the core are randomly oriented in space, *i.e.*, uncorrelated, which means that the total circulation energy for the core will be proportional to N_v rather than N_v^2. Thus, for large N_v the total circulation energy of the vorton core can be neglected relative to E_c. Consistent with the virial theorem, the energy E_c will exert a radial force tending to cause the vorton core to expand. As we show below, this expansion is opposed by a force deriving from dyangular momentum and energy.

2. Dyangular Momentum and Energy

Noether's theorem [40] dictates that the dyality invariance of Maxwell's equations, the Lorentz force, and their defining Lagrangian implies the existence of a conserved quantity associated with dyality rotation. This quantity is denoted here by L_d, which we shall call "dyangular momentum" to avoid confusion with ordinary angular momentum. L_d can be visualized as an angular momentum residing in the electromagnetic plane.

By analogy to classical mechanics we write

---

[18] It is tacitly assumed that the close proximity of the vortons in the core does not effect the quantum condition that leads the value of Q_0 given by Eq. (4). If it does, Q_0 should be replaced by $\overline{Q}_0'$, where $\overline{Q}_0'$ is an average value for the quantized vorton charge when residing in the vorton core. It is important to observe, however, that the essential features of the analysis leading to the equations governing the equilibrium configurations will be unaffected by this modification.

$$L_d = I_d \omega_d, \tag{43}$$

where I_d is the moment of inertia in dyality space. By the same analogy, the energy of dyality rotation will be given by

$$E_d = \frac{L_d^2}{2I_d}. \tag{44}$$

For guidance in finding a formula for I_d, we note that in classical mechanics the formula for the moment of inertia I of a point mass M is

$$I = r^2 M, \tag{45}$$

where r is the radius of gyration [5, p. 156]. Since the charges that are undergoing the dyality rotation have a Coulomb energy E_c, we use the Einstein relationship between energy and mass and designate

$$M_d = \frac{E_c}{c^2} = \frac{(N_v Q_0)^2}{R_c c^2} \tag{46}$$

as the relevant mass. Denoting the radius of gyration by $\lambda\!\!\!^{-}_{0_d}$, we write

$$I_d = k_I^2 \lambda\!\!\!^{-2}_{0_d} \frac{(N_v Q_0)^2}{R_c c^2}, \tag{47}$$

where $\lambda\!\!\!^{-}_{0_d}$ is a phenomenological parameter, the value of which presumably would derive from electromagnetism and dyality physics. (See **Sec. V. E**., above.) k_I is a factor (or function) presumably of order unity that is included to account for our ignorance about this aspect of vorton physics, *e. g.*, the extent of relativistic corrections, *etc*. From $\lambda\!\!\!^{-}_{0_d}$ one can define a fundamental dyality frequency.[19]

$$\omega_{0_d} \equiv c / \lambda\!\!\!^{-}_{0_d}. \tag{48}$$

Using these relationships, Eq. (47) can be simplified to

$$I_d = \frac{k_I^2 E_c}{\omega_{0_d}^2}. \tag{49}$$

---

[19] This definition differs from that in Ref. [11] in that we do not necessarily wish to tie $\lambda\!\!\!^{-}_{0_d}$ to the Compton wavelength of the photon. To avoid confusion, we have used a different subscript.

3. Equilibrium Point

We are now in a position to show (in lowest order) how the dyangular and Coulomb energies interact to yield a point of stable equilibrium for the size of the vorton core. To do this, we write the total energy of the vorton core

$$E_{tot} = E_c + E_d = E_c + \frac{\omega_{0_d}^2 L_d^2}{2k_I^2 E_c} = \frac{(N_v Q_0)^2}{R_c} + \frac{R_c}{2}\left(\frac{\omega_{0_d} L_d}{k_I N_v Q_0}\right)^2, \tag{50}$$

where N_v and L_d are initial conditions of the vorton core at the end of the dyality spinup process. The equilibrium value of R_c is determined by setting the derivative $dE_{tot}/dR_c = 0$, which shows that E_{tot} has a minimum at $E_c = E_d$. This minimum is a point of stable equilibrium for the configuration and satisfies the equation

$$R_c = \frac{\sqrt{2} k_I (N_v Q_0)^2}{\omega_{0_d} L_d}; \tag{51}$$

we extend this analysis in Sec. 4, below, by including a kinetic energy term.

We see that in this approximation the energy content and size of the MLO are expressed in terms of the two primary parameters N_v and L_d (recall that N_v and L_d are conserved). (One obtains the same equilibrium point as that for R_c by viewing E_c as the dependent parameter and setting $dE_{tot}/dE_c = 0$.) The nominal energy relationships of Eq. (50) are plotted in Fig. 4.

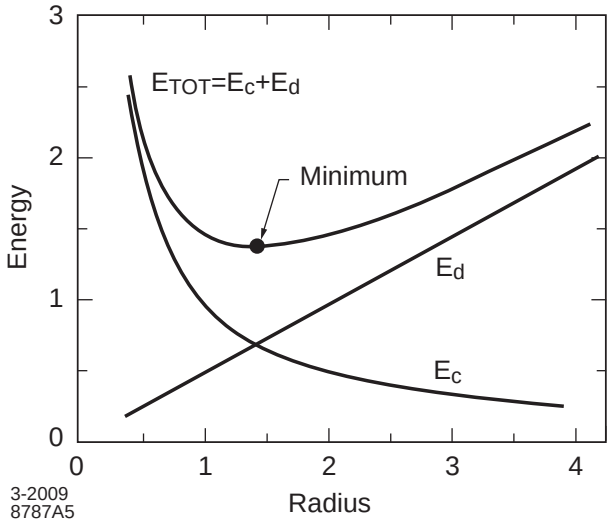

Figure 4: Depiction of total vorton energy $E_{tot} = E_c + E_d$ as a function of R_c.. (For simplification and ease of plotting we have set $N_v Q_0 = \omega_{0_d} L_d = k_I = 1$.) E_{tot} has a minimum at $E_c = E_d$, which in these units is located at $R_c = \sqrt{2}$. This is a point of stable equilibrium.

This counter-intuitive result obtains because, as indicated in Eq. (50), an increase in R_c entails an increase in dyangular energy. The essential result of this model, then, is that when L_d is large enough, the dyangular force is adequate to contain the Coulomb expansion force, and the localization and coherence of the vorton core is stably maintained without violating the virial theorem.

In looking more generally at this result, it can be seen that once the equilibrium condition (at the energy minimum) has been achieved, any fluctuation that tends to move a vorton or a collection of vortons a finite distance away from the spatial localization region or away from the (small) populated region in the phase space (Θ, ω_d) would increase

$$E_{tot} = E_{tot}(\chi_i), \tag{52}$$

where χ_i enumerates the coordinates of the relevant vortons or collections of vortons. Thus, as the configuration moves away from the equilibrium point, the equation

$$F_i = -\frac{\partial E_{tot}}{\partial \chi_i}, \tag{53}$$

where F_i is the force associated with the coordinate χ_i, dictates that F_i becomes negative. And $F_i < 0$ will act in such a way as to move the errant vortons back towards the equilibrium configuration.

A most interesting feature of this model is that in addition to the minimum of E_{tot} representing the single MLO/BL/EL, there can also be configurations that give local minima of E_{tot} and, hence, represent (meta)stable configurations. For example, consider a pair of vorton cores with coherent ω_d, as illustrated in Fig. 5. From the above discussion, one can see that such an equilibrium configuration will be characterized by

$$\frac{\partial E_{tot}}{\partial R_{c1}} = \frac{\partial E_{tot}}{\partial R_{c2}} = \frac{\partial E_{tot}}{\partial R_{21}} = 0. \tag{54}$$

Thus, using the same argument as above, we see that the dynamics of Coulomb energy and dyality rotation can not only account for the stability of the core in each of an orbiting pair configuration but also, at the same time, for the stability of the pair separation distance. And the stable pair separation distance can significantly exceed the size of the vorton cores. One can see that this argument

extends directly to multiple MLO/BL/EL configurations.[20] The relevance of Eq. (54) and its implications is found in Item 4) in **Secs. II** and **IV** above.

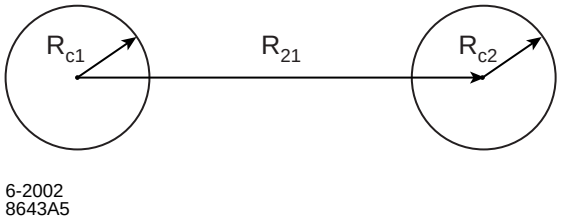

Figure 5: Depiction of a pair of vorton cores indicating the core radii R_{c1} and R_{c2} and the core separation distance R_{21}.

Finally, as an anticlimax, one expects that over the course of time, loss mechanisms would dissipate dyangular momentum and energy until L_d would be too small to effect this localization. Other forces, not included in this first-order approximation, would then become significant and disperse the vorton core(s).

4. Dyality Frequency at the Equilibrium Point

In the above approximation, it is easy to show the dyality frequency at the equilibrium point will be

$$\omega_{eq} = \frac{\sqrt{2}\omega_{0_d}}{k_I}. \tag{55}$$

A more detailed analysis that also includes a finite vorton temperature in the equilibrium energy equation was done in Ref. [11]. A nonzero temperature for the vorton core of MLO'S can be expected to result from the presence of the 1.5 GHz cavity drive power.[21] This power would generate a buildup of the (random or thermal) kinetic energy of the translational motion of the core vortons as a kind of a gas or plasma. In this case, the total energy will be

$$E_{tot} = E_c + E_d + E_k, \tag{50′}$$

where E_k is the total thermal (kinetic) energy of the constituent vortons. The equilibrium point of Eq. (50′) is found at [11, Eq. (C-8)]

[20] Of course, when R_{ci} and R_{ij} are comparable, the situation will be much more fluid, leading to the possibility of an adiabatic flow along a continuum of equilibrium configurations, all characterized by the same minimum of total energy. Some recent EL observations appear to be consistent with this analysis: "the light balls are not single objects but are constituted of many small components which are casually vibrating around a common barycenter. . . " [41].

[21] It is assumed that the proposed energy source for BL and EL, catalyzed nucleon decay [11], plays a negligible role in MLO'S and will not be discussed in this paper.

$$E_d = E_c + 3(\gamma - 1)\ E_k, \tag{56}$$

where $\gamma = c_p/c_v$ is the ratio of the specific heats of the vortons as a gas. Eq. (56) indicates that the dyangular force not only contains the expansion force of E_c but also that associated with E_k. As a result, ω_{eq} is also higher; assuming that $\gamma = 5/3$, the value for monatomic gases, we have [11, Eq. (C-10)]

$$\omega_{eq} = \frac{\omega_{0_d}}{k_I}\sqrt{2 + 4E_k / E_c}. \tag{55′}$$

A significant E_k content would have two additional consequences. First, since (an adiabatic) E_k varies inversely with the core volume, the tendency of E_k to maximize volume will promote a spherically symmetric shape for the vorton core. Second, it is natural to suppose that E_k could be characterized by a temperature sufficient to lead to visible thermal radiation. (One would also expect radiation from the recombination of electrons and ions, as well from excited ionic and atomic states.)

A more complete analysis can be made by including the electrons and ions residing in the vorton core along with its oscillating electric charge $N_v\ Q_0 \cos\ \omega_d t$. The charges of the electrons and ions will tend to cancel the electric charge of the vorton core, reducing the total electric Coulomb energy,

$$E_{C_e} = E_c \cos^2 \omega_d t + E_e + E_i + E_{ce} + E_{ci} + E_{ei}, \tag{57}$$

where the self-energies and the interaction energies are included using obvious notation. If the electric charge neutralization were complete, there would be no electric field and we would have $E_{C_e} = 0$. However, since the electric charge on the vorton core is oscillating, the net charge of the electrons and ions will also oscillate, never achieving a stable neutral equilibrium with the vorton core. Since the vorton core is the driving engine for the MLO, we can take all of the electric Coulomb physics processes into account by writing

$$E_{C_e} = \beta_e E_c, \tag{58}$$

where β_e is a time-dependent phenomenological parameter with a range $0 \le \beta_e \le 1$. Since the ions and electrons do not contribute to the magnetic Coulomb energy, one writes

$$E_{C_m} = E_c \sin^2 \omega_d t. \tag{59}$$

Using Eqs. (58) and (59), we can now take the presence of the electrons and ions into account in Eq. (50′) by using the substitution

$$E_c \Rightarrow E_{C_e} + E_{C_m} = (\beta_e + \sin^2 \omega_d t)E_c. \qquad (60)$$

The total energy, including electrons and ions, will then be

$$E_{tot} = (\beta_e + \sin^2 \omega_d t)E_c + E_d + E_k. \qquad (50'')$$

To set up the calculation to determine the equilibrium point, we note, that the E_c of Eq. (49) will be unaffected since the electrons and ions do not participate in dyality rotation. For this more general case deriving from Eq. (50″), then, at the equilibrium point one obtains

$$E_d = (\beta_e + \sin^2 \omega_d t)E_c + 3(\gamma - 1)E_k. \qquad (56')$$

Eq. (56′) is transcendental, meaning that ω_d will not be a constant during the (equilibrium) dyality cycle. Ignoring this subtlety, one can make a useful approximation by taking a time average over a dyality cycle to obtain

$$\overline{E}_d = (\overline{\beta}_e + ½)E_c + 3(\gamma - 1)E_k, \qquad (56'')$$

which, again setting γ = 5/3, leads to

$$\overline{\omega}_{eq} = \frac{\omega_{0_d}}{k_I}\sqrt{2\overline{\beta}_e + 1 + 4E_k / E_c}. \qquad (55'')$$

In the event that there are no electrons or ions present, we would have $\overline{\beta}_e = < \cos^2 \omega_d t > = ½,$ its maximum (average) value, retrieving the earlier results. At the other extreme, the electrons and ions significantly neutralize the electric charge of the core, and we have $\overline{\beta}_e \sim 0,$ leading to a lower value for $\overline{\omega}_{eq}$. In particular, if $\overline{\beta}_e = 0,$ and $E_k = 0$, we have $\overline{\omega}_{eq} = \omega_{0_d} / k_I$, about 30% less than the value given by Eq. (55). As E_k/E_c becomes larger, Eq. (55″) becomes a better approximation. In between these extremes, the accuracy of the approximation resulting from using the time average is enhanced because the time variation of $\beta_e(t)$ will tend to compensate for that of $\sin^2\omega_d t$.

VI. DISCUSSION

A. Qualitative Assessment

At this juncture, with the basic physics of the model in hand, it is of interest to look back at **Sec. II** to assess the qualitative explanatory power of the vorton model.

1) Luminosity. The 1.5 GHz cavity drive power can be expected to heat the vorton core, leading to thermal radiation. Radiation from electron-ion recombination and from excited ionic and atomic states would also be expected.

2) Motion Without Wall Contact. The vorton core is a self-contained stable system and does not need a current injection from a conductor to sustain it.

3) Long Range Force. One expects the magnetic charge on the vorton core to develop image charges of the same polarity in the walls of the superconducting niobium cavity. The repulsion between like magnetic charges will act to maintain the MLO (or the multi-MLO configuration) in the central region of the cavity.

4) Stable Configurations of Multiple MLO'S. Minimization of the total energy of the configuration sets the equilibrium condition for both the MLO cores and separation distances between MLO'S. And the stable separation distance can exceed the MLO sizes.

5) Long Lifetime. Dyality symmetry and the conservation of L_d furnish the physics basis for a long MLO lifetime.

6) and 7) Self-Coherence. Dyangular momentum and energy acting through the equilibrium condition furnish the self-coherence forces.

From this assessment, it appears that the vorton model shows considerable promise. This assessment could be improved by experimental observation of optical spectra of the MLO, *cf.* Item 8) in **Sec. IV**, above.

B. Dyality Frequency

While there are, as of yet, no measurements that give clear evidence of dyality rotation or the dyality frequency (*e. g.*, the direct observation of an oscillating electric or magnetic field), there are aspects of existing data that appear to support these concepts. These examples indicate that the frequency of dyality rotation $f_d = \omega_d/(2\pi)$, when it is associated with the BL type objects (to include MLO's and EL's), is generally at a fairly low frequency.

One example, which will be the topic of a forthcoming paper [42], is found in observed aspects of the MLO orbits, as discussed in Ref. [2]. As a prelude, we note that the presence of elliptical (or quasi-elliptical) orbits was taken as supporting evidence for the relevance of the SPM in MLO behavior. It was detailed in Ref. [2] that precession of the elliptical shape was also generally observed, and that the precession direction correlated in (almost) all cases with the orbital direction, even when the orbital direction reversed sense (a reversal of the orbital L_z). In the SPM model, the explanation for this correlation derives

from the fact that in the cavity the magnitude of the ***E*** field diminishes as one moves in the equatorial plane away from the center of the cavity. As discussed in Ref. [42], an orbital rocking motion (sequential cycles of precession reversal) is possible when the frequency of dyality rotation synchronizes with the orbital frequency. (The oscillating magnetic charge interacts with a small residual transverse magnetic field in the cavity, in turn augmenting and diminishing the orbital L_z.) A clear example of such rocking motion was also seen in Orbit 10 (an orbit of ~15 s duration) of Ref. [2]. Thus, the observed orbital frequency of 6.7 Hz for that orbit indicates a frequency of dyality rotation of 6.7 Hz, a relatively low frequency.

In addition, having made the case that this model comprehends the MLO/BL/EL phenomena, it is appropriate to use data from any one of these sub-phenomena as useful input. In this regard, it is of interest to point out that there is a photograph taken in 1984 at Hessdalen [18] in which the track of an EL was observed to oscillate with a frequency of 7 ± 2 Hz. This photograph is reproduced in Fig. 6. A straightforward interpretation would be that the electromagnetic charge of the EL, performing dyality rotation with $f_{eq} \sim 7$ Hz, was interacting with a local static electric or magnetic field. If, for example, the oscillation of the EL track were due to a magnetic Coulomb interaction with the earth's ***B*** field, one could attribute the onset of the oscillations to a rising trajectory, which would reduce atmospheric viscous damping [22] as the air became thinner with higher altitude.[23]

This Hessdalen result, and the Orbit 10 discussion above, indicates that f_{eq} is a fairly low frequency, about 7 Hz in these examples. As shown by Eq. (55′), $f_{0_d} = \omega_{0_d} / (2\pi)$ would be even lower, depending upon the importance of E_k. It was suggested in Ref. [11] that the ω_{0_d} may derive from a possible photon mass[24] rather than a kind of fundamental dyality mass, as suggested above.

It should be possible to actually determine directly the f_{eq} in a cavity lights experiment by a direct measurement of the ***B***′ fields as described in the next section. Until such a measurement is made, we shall have to rely on the orbital analysis above, and the assumed correlation between the orbital rotation frequency and the dyality frequency of the electromagnetic charge of the MLO.

---

[22] The role of viscous forces in these phenomena appears to be of some significance and is currently being investigated.

[23] Immediately subsequent to the photograph, witnesses at the scene observed that the amplitude of the EL oscillations continued to increase and the EL quickly disappeared [43]. This observation is consistent with the rising trajectory hypothesis, which would entail a continuous reduction of viscous forces.

[24] The best present limit on the photon mass is $\leq 8\times10^{-16}$ eV/c^2 or $f_0 \leq 0.2$ Hz [44].

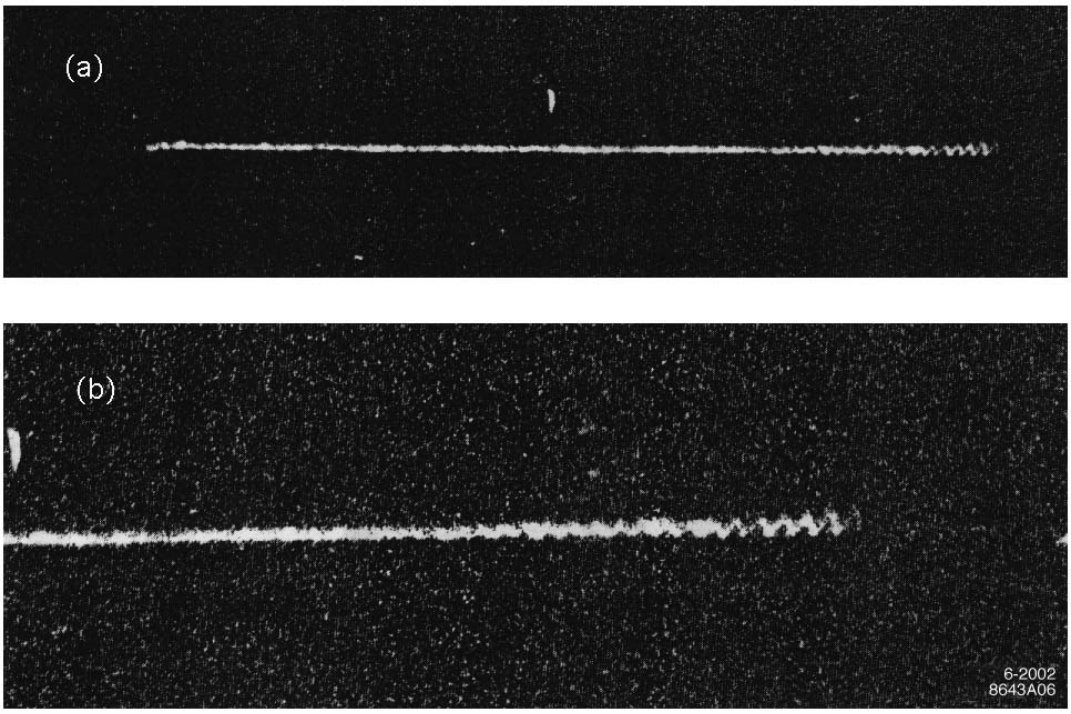

Figure 6: Ten second time exposure photograph of an EL taken in 1984 at Hessdalen. The oscillation of the path, moving from left to right, is at a frequency of 7 ± 2 Hz.

C. The Magnetic Field B' and Vacuum Currents

Before discussing the measurement of $\boldsymbol{B}'$, it is relevant that we make a short digression. The vacuum currents associated with dyality rotation lead to an interesting experimental prediction, which might be called the "no-eddy-current" effect. As an aid to visualize this effect, imagine a circular loop of radius b is placed at a distance d from a localized electromagnetic charge density ρ_0 at the origin, as depicted in Fig. 7. We define $Q \equiv \iiint \rho_0 d\boldsymbol{x}$ and, assume that Q is performing a dyality rotation at a frequency ω_d. Hence, the magnetic component of this charge will vary with time, and is given by

$$Q_m = Q \sin \omega_d t. \tag{61}$$

By Eq. (14), the original magnetoelectric Maxwell's equations, we expect a (radial) magnetic field

$$\boldsymbol{B}' = \frac{Q \sin \omega_d t \ \mathbf{1}_r}{d^2} \tag{62}$$

at the loop. This field would induce an electric field gradient in the loop equal to

$$\mathcal{E}'_B = -\frac{bQ\omega_d}{2cd^2}\cos\omega_d t. \tag{63}$$

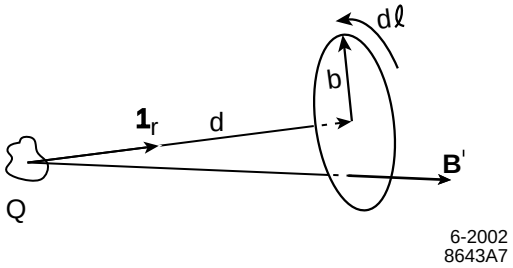

Figure 7: A loop of radius *b* placed at a distance *d* from the origin where a charge of magnitude *Q* is undergoing dyality rotation. The unit radial vector $\mathbf{1}_r$ is indicated. The direction of the unit area vector of the loop is parallel to $\mathbf{1}_r$ at the center of the loop, and the direction of the incremental distance $d\ell$ of the associated line integral around the loop is indicated.

However, Eq. (35′) dictates that the $\oint \mathcal{E}'_B d\ell$ around the loop from the $d\boldsymbol{B}'/dt$ through the loop (due to the oscillating magnetic charge) is exactly cancelled by an equal and opposite $\oint \mathcal{E}'_g d\ell$ from the radial $\boldsymbol{g}_v$ through the loop, which coherently oscillates with $\boldsymbol{B}'$. That is, the radial $\boldsymbol{B}'$ is building up at the loop because the $\boldsymbol{g}_v$ flowing inward is augmenting Q_m. With no net induced voltage around the loop, no induced current will flow in the loop. It follows that even if the loop were replaced by a sheet of perfectly conducting material, by the same argument, no eddy currents would flow in this sheet. As a consequence, the (oscillating) magnetic field (and its associated oscillating vacuum current $\boldsymbol{g}_v$) resulting from the dyality rotation of charge would penetrate this perfect conductor as though it were not there.

Let us now consider whether or not the $\boldsymbol{B}'$ field and its associated current $\boldsymbol{g}_v$ can, by the same line of reasoning, penetrate a superconductor, which is indeed a perfect conductor. In considering this question, it is relevant to observe that in addition to being a perfect conductor, *i.e.*, $\boldsymbol{E} = 0$ in the interior of the superconductor, superconductors also exhibit the Meissner effect, which requires that $\boldsymbol{B} = 0$ in the interior of the superconductor. As the temperature is lowered through the critical temperature T_c, it becomes energetically possible for a condensate of Cooper pairs to form (if $\boldsymbol{B} = 0$ inside the superconductor [45]). When the external magnetizing force $\boldsymbol{H}_{ext}$ is nonzero, but not too large, the energy available from this condensation is enough to reject the interior magnetic field (and its associated energy). It is this condensation, then, that leads to the Meissner effect and an interior $\boldsymbol{B} = 0$. When $\boldsymbol{H}_{ext}$ becomes large enough, the available magnetic energy exceeds the condensation energy, and the material

becomes normal again.[25] From a thermodynamical point of view, the material is seeking a state of lowest Gibbs free energy [47]. Presumably, these energy considerations are also valid for the $\boldsymbol{B}'$ field of the vortons. And once the $\boldsymbol{B}'$ field cannot exist in the interior of the superconductor, then the associated current $\boldsymbol{g}_v$ will be shunted away by reactionary supercurrents. Thus, one expects that both the $\boldsymbol{B}'$ and $\boldsymbol{g}_v$ will be shunted out the ends of the cavity, penetrating the vacuum flanges, which are made of normal metal (typically a stainless steel alloy). One notes that when one considers such a path through normal material, even though that path is enclosed by a superconductor, the no-eddy-current effect will obviate the flux quantization of the $\boldsymbol{B}'$ field.[26]

A prediction of this theory, then, is that an oscillating magnetic field with a fairly low frequency could be detectable outside the cavity when MLO'S are visible inside. (The no-eddy-current effect, however, would dictate that a pickup loop would not detect this field; a fluxgate magnetometer should be used.) The highest field level of this signature will be near the flanges at the ends of the cavity; the maximum magnitude of this field will be $N_v Q_0/R^2$, where R is the (effective) distance from the MLO to the magnetic sensor. Tantalizing hints of such fields at the 10^{-5} Gs level were reported in Ref. [2], but these observations are at the limit of sensitivity of the fluxgate magnetometer, and it is not clear that they were not due to some related background effect. Clearly, additional data is needed to resolve this question.

It should also be noted that the deflection of the $\boldsymbol{B}'$ fields away from the interior walls of the superconducting cavity can be described in the usual way by magnetic image charges in the cavity walls. Since these image charges will be of the same sign as the source magnetic charge, $N_v Q_0 \sin\theta$, one has at once an explanation for the long-range axial stabilizing force that the existing data calls for, but which the SPM could not provide.

VII. SUMMARY AND CONCLUSIONS

In this paper the properties of MLO'S, as observed, were reviewed. A striking aspect of the MLO'S data was that the MLO performed closed orbits without wall contact for extended periods of time inside a superconducting niobium cavity. A small particle model was described. The SPM was able to account for important aspects (*e. g.*, radial stability and a preference for an elliptical shape) of these orbits, but it was asserted that no explanation for the observed axial stability of

---

[25] For Type II superconductors like niobium, flux penetration starts at $H_{c1} < H_{c2}$; H_{c2} indicates the field strength at which the material becomes normal throughout. For niobium at $T = 0$, $H_{c2} =$ 1950 Oersteds [46].

[26] Presumably, some fraction of the $\boldsymbol{B}'$ and its associated $\boldsymbol{g}_v$ could also thread through the (normal) fluxon tubes trapped in the superconducting niobium, but the very small radius of these tubes would tend to keep this fraction quite small.

these orbits was evident. Another important question relative to the MLO data was the nature of the objects themselves. Analysis based upon the SPM appears to rule out ordinary matter in its known states: solid, liquid, or gas. And looking to a plasma MLO as the answer leads to an apparent violation of the virial theorem; *i, e.*, no answer there either. The need for proper understanding of these questions leads to the conclusion that the SPM is incomplete and forms the basis of the argument that the MLO phenomena cannot find an explanation within the realm of established physics.

Noting that the qualitative features of MLO'S are very much like those of BL (and EL), a BL model that incorporates electromagnetic charge performing dyality rotation was described. It was pointed out that the magnetic charge intrinsic to this BL model could furnish an axial stabilizing force. In addition, the process of dyality rotation gives rise in a natural way to a force that could contain the Coulomb and thermal energies of the MLO'S and hence satisfy the virial theorem. Thus, while the MLO/BL/EL model has the capability of explaining the most perplexing aspects of the MLO data, its foundations reside outside the realm of presently established physics.

In conclusion, in view of the obvious limitations of established physics to explain the data in hand, it is important that as additional cavity lights data becomes available, the explanatory power of the new physics framework offered by the vorton BL model be further explored.

VIII. ACKNOWLEDGEMENTS

I would like to thank J. Mammosser, P. Anthony, M. Sullivan, J. Weisend and I. Wieder for numerous useful conversations. Also, I would like to thank J. Mammosser, C. K. Sinclair, and I. Wieder for some important references.

REFERENCES

[1] J. R. Delayen and J. Mammosser, *Proceedings of the 1999 Particle Accelerator Conference*, New York, p. 925.

[2] P. L. Anthony, J. R. Delayen, D. Fryberger, W. S. Goree, J. Mammosser, Z. M. Szalata, and J. G. Weisend II, *Submitted for publication*.

[3] D. Fryberger, *Nuc. Inst. Meth*., **A459**, 29 (2001).

[4] Y. Han and L. C. Biedenharn, *Nuovo Cimento*, **2A**, 544 (1971).

[5] H. Goldstein, *Classical Mechanics* (Addison-Wesley Publishing Co., Inc., Reading, MA and London, 1950), p. 69.

[6] C. L. Longmire, *Elementary Plasma Physics* (Interscience Publishers, New York, 1963), p. 68.

[7] J. D. Jackson, *Classical Electrodynamics*, (J. Wiley & Sons, Inc., New York and London, 1962).

[8] B. M. Smirnov, *Usp. Fiz. Nauk*, **161**, 141 (1991) [*Sov. Phys. Usp*., **34**, 711 (1991)].

[9] V. L. Bychkov, *Phil. Trans. R. Soc. Lond. A*, **360**, 37 (2002).

[10] J. Abrahamson and J. Dinniss, *Nature*, **403**, 519; J. Abrahamson, *Phil. Trans. R. Soc. Lond. A*, **360**, 61 (2002).

[11] D. Fryberger, "A Model for Ball Lightning," *Proceedings of the First International Workshop on the Unidentified Atmospheric Light Phenomenon in Hessdalen* (March 23-27, 1994), Østfold College Report 1997:5/Part I.

[12] S. Singer, *The Nature of Ball Lightning* (Plenum Press, New York, 1971).

[13] J. D. Barry, *Ball Lightning and Bead Lightning* (Plenum Press, New York, 1980).

[14] Y.-H. Ohtsuki, Ed., *Science of Ball Lightning* (World Scientific, Singapore, 1989).

[15] M. Stenhoff, *Ball Lightning* (Klewer Academic/Plenum Publishers, New York, Boston, Dordrecht, London, and Moscow, 1999).

[16] W. R. Corliss, *Lightning, Auroras, Nocternal Lights, and Related Luminous Phenomena* (The Sourcebook Project, Glen Arm, MD, 1982).

[17] G. Endean, *Proc. of the 6th Int. Symp. on Ball Lightning*, Antwerp, Belgium (Aug. 1999), p. 53.

[18] E. Strand, *Project Hessdalen* 1984, *Final Technical Report, Part One*.

[19] P. Deveraux, *Earth Lights* (Turnstone Press, 1982); *Earth Lights Revelation* (Blanford Press, London, 1989).

[20] G. Dijkhuis, "Statistics and Structure of Ball Lightning," *Proceedings of 3rd Int. Ball Lightning Symp.*, S. Singer, Ed., In Press.

[21] J. C. Maxwell, *A Treatise on Electricity and Magnetism* (3rd Ed., Oxford University Press, London, 1892).

[22] S. Shanmugadhasan, *Can. J. Phys.* **30**, 218 (1952); N. Cabibbo and E. Ferrari, *Nuovo Cimento*, **123**, 1147 (1962).

[23] Oliver Heaviside, *Electromagnetic Theory* (Chelsea Publishing Co., London, 1893).

[24] G. Y. Rainich, *Trans. Am. Math. Soc.*, **27**, 106 (1925).

[25] D. Fryberger, *Found. Phys*., **19**, 125 (1989); *Found. Phys. Lett.*, **3,** 375 (1990).

[26] D. Fryberger, *Had. Jour*., **4**, 1844 (1981).

[27] R. Davis and E. P. S. Shellard, *Phys. Lett. B*, **209**, 485 (1988).

[28] A. Vilenkin and E. P. S. Shellard, *Cosmic Strings and Other Topological Defects* (Cambridge Univ. Press, Cambridge, 1994).

[29] E. Cunningham, *Proc. Lond. Math. Soc*., **8**, 77 (1910); H. Bateman, *Ibid*., 223.

[30] Y. Murai, *Prog. Theor. Phys. (Kyoto)*, **9**, 147 (1953).

[31] P. M. Morse and H. Feshbach, *Methods in Theoretical Physics* (McGraw Hill Book Co., New York, 1953), p. 666; H. Bateman, *Partial Differential Equations of Mathematical Physics* (Cambridge Univ. Press, Cambridge, 1959), p. 461.

[32] R. Penrose and W. Rindler, *Spinors and Space-Time, Vol. 2* (Cambridge University Press, Cambridge, New York, and Melborne, 1988), p. 62.

[33] P. A. M. Dirac, P*roc. Roy. Soc.*, **A133**, 60 (1931); *Phys. Rev.*, **74**, 817 (1948).

[34] H. Padamsee, J. Knobloch, and T. Hayes, *RF Superconductivity for Accelerators* (John Wiley & Sons, Inc., New York, Chichester, Weinheim, Bisbane, Singapore, and Toronto, 1998), p. 235 *et seq*; H. Padamsee and J. Knobloch, "The Nature of Field Emission From Microparticles and the Ensuing Voltage Breakdown," *AIP Conference Proceedings 474, '98 RF Conference, Pajaro Dunes, CA* (Am. Inst. of Physics, Woodbury, NY, 1999), p. 212.

[35] J. Knobloch, "Advanced Thermometry Studies of Superconducting Radio-Frequency Cavities," Ph.D. Thesis for Cornell University, 1997.

[36] E. Amaldi, "On the Dirac Magnetic Poles," in *Old and New Problems in Elementary Particles*, G. Puppi, Ed. (Academic Press, New York and London, 1968).

[37] E. Katz, *Am. J. Phys.* **33,** 306 (1965).

[38] J. D. Jackson, *Classical Electrodynamics*, 2nd Ed. (John Wiley & Sons, New York, Chichester, Brisbane, Toronto, Singapore, 1975), p. 252.

[39] T. K. Simpson, M*axwell on the Electromagnetic Field* (Rutgers Univ. Press, New Brunswick, New Jersey, and London, 1997).

[40] E. Noether, *Nachr. kgl. Ges. Wiss.* Götingen, 171 (1918); E. L. Hill, R*ev. Mod. Phys.*, **23,** 253 (1951).

[41] M. Teodorani, E. P. Strand, B. G. Hauge, *EMBLA 2001: The Optical Mission* at www.itacomm.net/PH, Oct. 2001.

[42] D. Fryberger, *In Preparation.*

[43] E. Strand, *Private Communication*.

[44] E. Fischbach, H. Kloor, R. A. Langel, A. T. Y. Lui, and M. Peredo, *Phys. Rev. Lett.*, **73**, 514 (1994).

[45] H. Fröhlich, *Proc. Phys. Soc. A*, **168**, 129 (1951).

[46] D. R. Tilley and J. Tilley, *Superfluidity and Superconductivity* (John Wiley & Sons, New York, 1974), p. 13.

[47] M. Tinkham, I*ntroduction to Superconductivity*, 2nd Ed. (McGraw Hill, Inc., New York, St. Louis, San Francisco, 1996), p. 22, *et seq.*

FIGURE CAPTIONS

Figure 1: Schematic depiction of the structure of the vorton. The basic underlying toroidal coordinate system is evident. The arrows denote the simultaneous "rotations" or charge flux lines in ϕ and ψ, which are associated with L_ϕ (around the *z*-axis or $\sigma = 0$) and L_ψ (around the ring of radius *a*, *i.e.*, $\sigma = \infty$, which sets the scale of the toroidal system). One can see that the charge flux lines, as indicated by the arrows, all lie in the surface of one of the (nested) tori and are in the sense of increasing ϕ and ψ. By definition, this configuration carries positive topological charge.

Figure 2: The electromagnetic or dyality plane with electric and magnetic axes is shown. The circle of radius Q_0 (equivalent to 25.83 *e*), the magnitude of the (ground state) vorton's generalized electromagnetic charge, is also shown. This circle is called the dyality circle, and any point on this circle, designated by its dyality angle Θ, is a possible value for the vorton charge. A $Q = Q_0$ at $\Theta = 30°$ is indicated. For orientation, the electron *e*, the proton *p*, and the iron nucleus Fe ($Z = 26$) are plotted. If the vorton charge is in a state of dyality rotation of angular velocity ω_d, then $\omega_d = d\Theta/dt$, as depicted in the figure.

Figure 3: a.) Illustration of the rotation of the electromagnetic plane by the angle $\Theta = 30°$. The same charge *Q* has new electromagnetic components in the rotated plane. b.) Rotation of electromagnetic charge by the same angle $\Theta = 30°$. The rotated charge Q^R has new electromagnetic components in the (same) dyality plane.

Figure 4: Depiction of total vorton energy $E_{tot} = E_c + E_d$ as a function of R_c.. (For simplification and ease of plotting we have set $N_v Q_0 = \omega_{0_d} L_d = k_I = 1$.) E_{tot} has a minimum at $E_c = E_d$, which in these units is located at $R_c = \sqrt{2}$. This is a point of stable equilibrium.

Figure 5: Depiction of a pair of vorton cores indicating the core radii R_{c1} and R_{c2} and the core separation distance R_{21}.

Figure 6: Ten second time exposure photograph of an EL taken in 1984 at Hessdalen. The oscillation of the path, moving from left to right, is at a frequency of 7 ± 2 Hz.

Figure 7: A loop of radius *b* placed at a distance *d* from the origin where a charge of magnitude *Q* is undergoing dyality rotation. The unit radial vector $\mathbf{1}_r$ is indicated. The direction of the unit area vector of the loop is parallel to $\mathbf{1}_r$ at the center of the loop, and the direction of the incremental distance $d\ell$ of the associated line integral around the loop is indicated.